Journal of Nuclear Materials xxx (2013) xxx–xxx

Contents lists available at SciVerse ScienceDirect

Journal of Nuclear Materials

journal homepage: www.elsevier.com/locate/jnucmat

Interaction of dislocations with Frank loops in Fe–Ni alloys and pure Ni: An MD study

D. Terentyev [a,*], A. Bakaev [a,b], Yu.N. Osetsky [c]

[a] SCK-CEN, Nuclear Material Science Institute, Boeretang 200, B-2400 Mol, Belgium
[b] Center for Molecular Modeling, Department of Physics and Astronomy, Ghent University, Technologiepark 903, 9052 Zwijnaarde, Belgium
[c] Materials Science and Technology Division, ORNL, Oak Ridge, TN 37831, USA

ARTICLE INFO

Article history:
Available online xxxx

ABSTRACT

Variation of the stacking fault energy in FCC alloys and austenitic steels is well known to influence the evolution of radiation damage and its effect on deformation mechanisms. The primary defects observed in austenitic steels under neutron irradiation are mainly Frank loops. Here, we study the interaction of edge and screw dislocations with Frank loops in low stacking fault energy Fe–Ni alloys. The interatomic potentials employed were specially developed to reproduce a number of properties of real austenitic steels. The influence of temperature and loop morphology on the interaction mechanism and the critical resolved shear stress for dislocations to overcome loops has been investigated. All investigated reactions have been subdivided into three classes depending on temperature, loop size and interaction geometry. It is shown that by decreasing stacking fault energy below a certain value the formation of constrictions on dislocations is suppressed so that loop unfaulting becomes a less favorable mechanism in comparison with loop shear. Additional effect of solid-solution alloying, causing a non-negligible friction stress, is expressed in the impedance of the propagation of dislocations in the secondary glide planes, which is another factor limiting the unfaulting process.

1. Introduction

Plasticity of metals and metallic alloys is known to be controlled by the movement of dislocations [1]. Irradiation of metals, metallic alloys and steels by energetic particles causes modification of the crystal microstructure resulting in the formation of new lattice defects such as precipitates, dislocation loops and voids [2]. These defects act as obstacles to dislocation glide, thereby causing hardening and consequently embrittlement [1,2]. In the case of neutron irradiation (of structural and in-core reactor components at temperature below $0.3T_M$), the matrix damage created is composed mainly of dislocation loops (see e.g. [3]). Interaction of moving dislocations with loops is therefore an important contribution to plastic deformation mechanisms in irradiated crystalline materials, as was directly revealed by transmission electron microscopy studies (for FCC metals see e.g. [4–6]).

In FCC metals, alloys and austenitic stainless steels, which are subject of the present work, both faulted Frank loops (FLs) with Burgers vector (BV) $1/3\langle 1\,1\,1\rangle$ and perfect unfaulted loops with BV $\frac{1}{2}\langle 1\,1\,0\rangle$ form under irradiation [1]. Due to the low stacking fault energy (SFE) of austenitic alloys, FLs are a major component of the microstructure formed under neutron irradiation [7]. The interaction of FLs with dislocations has already been studied by Molecular Dynamics (MD) simulations in pure FCC Ni and Cu. A systematic study performed by Nogaret et al. [8] has revealed several mechanisms depending on the interaction geometry and impinging dislocation character. The following three mechanisms have been identified: (i) loop shearing; (ii) loop unfaulting into glissile configuration; (iii) loop absorption into glissile superjogs (on edge dislocations) or helical turns (on screw dislocations). For both screw and edge dislocations the unfaulting mechanism is controlled by a cross-slip process. In general, the number of geometrical configurations leading to loop unfaulting is higher for a screw dislocation [8].

In the case of a screw dislocation two distinct unfaulting mechanisms have been revealed [8,9]: (i) the formation of a D-Shockley partial dislocation segment, which sweeps the fault. The sweeping is accommodated by cross-slip of the dislocation around the loop. (ii) Cross-slip of the dislocation, formation of a constriction and its re-dissociation in the loop habit plane. Then, two partials remove the fault. Both of these mechanisms require the formation of constrictions and propagation of dislocations in the secondary glide planes. Note that cross-slip dislocation movement, also occurring by means of the constriction formation and being directly related to SFE of a material, plays a crucial role in the process of work-hardening [1].

The previous studies were performed for pure Ni and Cu, due to the lack of reliable interatomic potentials for austenitic steels (i.e.

* Corresponding author. Tel.: +32 014 33 31 97.
E-mail address: dterenty@sckcen.be (D. Terentyev).

0022-3115/$ - see front matter © 2013 Elsevier B.V. All rights reserved.
http://dx.doi.org/10.1016/j.jnucmat.2013.01.328

Cu has relatively low SFE but also too low shear modulus, while Ni has comparable shear modulus but very high SFE). Recently, however, an Fe–Ni interatomic potential set has been developed specifically to reproduce both shear modulus and SFE comparable to those of austenitic stainless steels [10]. In this work, we apply this potential to study the interaction of FLs with dislocations in Fe–Ni solid solutions containing 50 at.% and 70 at.% Ni. The choice of these two compositions was governed by the desired value of SFE (i.e. to be in the range of that relevant for austenitic steels) and full stability of FCC phase. We also perform simulations of pure Ni using two different potentials predicting low and high SFE. In this way, we attempt to make a step further towards understanding the effect of low SFE on dislocation-loop interaction.

The effect of alloying (i.e. variation of SFE, shear modulus and dislocation friction stress) on dislocation-FL interaction mechanisms is also addressed in this work. We show that by decreasing SFE below a certain value the formation of constrictions is suppressed so that unfaulting becomes a less favorable mechanism in comparison with loop shear. Furthermore, the presence of a non-negligible friction stress may also impede the propagation of dislocations in the secondary glide planes, which is an essential factor suppressing the unfaulting process that has not been reported so far.

2. Simulation details

The interaction of dislocations with FLs has been studied for pure Ni and Fe–50Ni and Fe–70Ni random alloys. The Fe–Ni potential was specifically developed to mimic properties of 316 austenitic steels and was parameterized using a wide range of data including some obtained by *ab initio* calculations [10]. The potential has the standard Embedded Atom Method (EAM) form [11], which offers a reasonable compromise between computing speed and reliability. For random alloys, the potential predicts an FCC structure to be more stable than BCC if Ni content exceeds 40 at.% [10]. The stacking fault energy increases smoothly from 0 to 125 mJ/m^2 with increasing Ni content, as shown in Fig. 1. In Fe–50Ni, SFE is about 15 mJ/m^2, which is in the range of the lowest values for austenitic steels [12], while in Fe–70Ni it rises to 50 mJ/m^2, which represents an upper bound.

To perform the simulations of pure Ni, we applied two EAM potentials developed by Mishin [13] (henceforth M-potential) and Voter [14] (henceforth V-potential). The M-potential is the basis of the Fe–Ni potential used here, while the latter was often used in the past to study behaviour of lattice defects in Ni. The basic properties of these potentials are summarized in Table 1. The V-potential predicts SFE = 58 mJ/m^2 which is close to that of the Fe–70Ni. The M-potential provides twice as high value of SFE in pure Ni. The shear modulus of Fe–50Ni and Fe–70Ni alloys is close to that of austenitic steels.

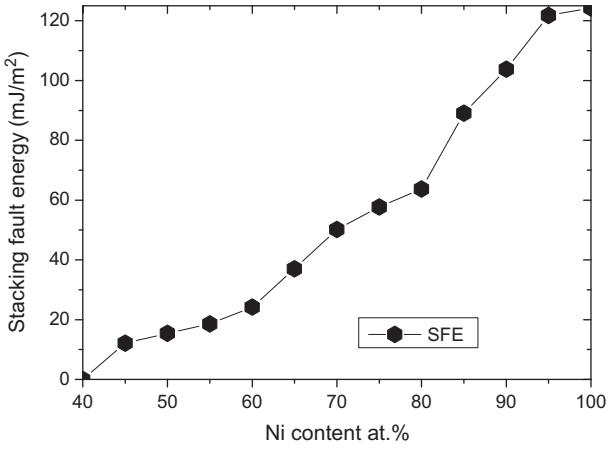

Fig. 1. Evolution of SFE as a function of alloy composition.

The interaction between dislocations and loops was studied using a classical MD approach [15] applying the so-called method of 'periodic array of dislocations' [16]. A pure shear deformation $[1\,1\,0]$ $(\bar{1}\,1\,1)$ with a constant strain rate (10^6 s^{-1}) was used to initiate the movement of a dislocation at a desired velocity, with other relevant details found in Ref. [16]. The model, with axes oriented along $[1\,1\,0]$, $[1\,\bar{1}\,2]$ and $[\bar{1}\,1\,1]$ directions, contained about 1.2 M mobile atoms and dimensions along x, y and z were $84 \times 62 \times 52 * a_3^0$ (where a_0 was chosen appropriately to account for thermal expansion). Periodic boundary conditions were applied along x and y directions, while atoms in a few outer $\pm z$ atomic layers were rigidly fixed in their perfect crystal positions. Screw and edge dislocations with $\boldsymbol{b} = 1/2[1\,1\,0]$ have been introduced and relaxed. Both types of dislocations dissociated in the $(\bar{1}\,1\,1)$ plane into two Shockley partial dislocations during relaxation.

An FL was introduced 10 nm away from the leading partial dislocation so that its geometrical centre coincided with the dislocation glide plane. The four non-equivalent orientations of BV were inspected. We have considered regular hexagonal FLs with sides oriented along $\langle 1\,1\,2\rangle$ and $\langle 1\,1\,0\rangle$ directions and diameter of 4 nm. Due to the imposed periodic boundary conditions along the dislocation line, the centre-to-centre spacing between the loops was 28 nm.

Integration of Newton's equations was performed using a constant time step equal to 2 fs. Calculations were done in the framework of a microcanonical NVE ensemble (see e.g. [15]), where atom number, N, system volume, V, and total energy, E, are conserved if the work of external forces is taken into account. Most of the simulations were done at 300 K and some additional ones at 600 K and 900 K. The initial temperature was achieved applying the Maxwellian distribution to the atoms in the model, which was equilibrated for 10 ps to prior to applying the constant strain rate deformation. The identification of the dislocation core and stacking fault atoms was realized by applying a combination of methods, namely: central symmetry analysis, common neighbour analysis, potential energy analysis and counting specific number of FCC neighbours.

3. Results

3.1. Interaction mechanisms

Based on the main set of MD simulations performed at 300 K for loops of 4 nm size, we distinguished three basic interaction mechanisms: (i) loop shear, (ii) loop absorption and (iii) loop unfaulting

Table 1
Lattice properties predicted by different interatomic potentials for pure Ni and Fe–50Ni and Fe–70Ni solid solutions. SFE in the Fe–Ni alloys was computed by considering 250 A^2 as a surface of the stacking fault and by performing 100 relaxation runs sampling the spatial distribution of solutes.

	Pure Ni: potential M	Pure Ni: potential V	Fe–50Ni	Fe–70Ni
a_0 (Å) Lattice unit	3.52	3.52	3.7	3.66
E_c Cohesive energy (eV/atom)	−4.45	−4.45	−4.40	−4.44
E_v^f (vacancy formation energy (eV)	1.60	1.56	1.63	1.62
E_i^f $\langle 1\,0\,0\rangle$-dumbbell formation energy (eV)	4.93	4.70	4.7	4.56
Shear modulus (GPa)	147	71	81.2	93.5
SFE (mJ/m^2)	125	58	15	50

prior to contact with the dislocation line. Fig. 2 summarizes schematically the reaction outcome depending on the material and interatomic potential at 300 K. We see that in low SFE Ni and Fe–50Ni models, the main interaction mechanism is shear. While in high SFE Ni – it is unfaulting and absorption. Hence, a decrease of SFE enhances the shear of loops. In the Fe–50Ni alloy, there is only one configuration where the FL is completely absorbed into the screw dislocation (SD) line (see Fig. 2a). In the following we briefly describe the interaction mechanisms and differences observed in the reactions performed in the Fe–50Ni solid solution and in pure Ni.

As discussed in [8,9], a screw dislocation is more efficient than an edge dislocation at absorbing FLs. Two examples of reactions between a screw dislocation and FLs with sides oriented along $\langle 1\,1\,0\rangle$ directions and $\boldsymbol{b} = 1/3[1\,1\,\bar{1}]$ and $1/3[1\,1\,1]$ are visualized in Figs. 3 and 4, respectively. A brief description of the interaction mechanisms is provided in the captions. The same reactions were modelled in pure Cu [8] and in Ni [9] and absorption via cross-slip movement was observed. Here, we observed loop absorption only in pure Ni (with both potentials) and Fe–70Ni, while in the low SFE alloy (i.e. Fe–50Ni), the cross-slip movement was suppressed and for $1/3[1\,1\,1]$ loop shear has occurred instead.

Two possible reasons led to the absence of absorption in these two cases. Absorption requires cross-slip, but the absence of a constriction during the interaction (see Fig. 4) does not allow for cross-slip and the corresponding sweeping up of the stacking fault. In contrast, a constriction was formed in the reaction shown in Fig. 3, but the constriction did not propagate across the loop surface, unlike in the reaction modelled in pure Cu or Ni. The mechanism that suppresses such propagation may be attributed to a significant lattice friction arising from the presence of solute atoms.

Finally, the mechanism referred to as 'Unfault before reaction' (see Fig. 2), occurs when the approaching dislocation initiates nucleation and propagation of two Shockley partial dislocation segments on the loop surface. The partials sweep across the extrinsic fault transforming an FL into a perfect loop ($\boldsymbol{b} = \frac{1}{2}\langle 1\,1\,0\rangle$). This unfaulting mechanism was observed for both screw and edge dis-

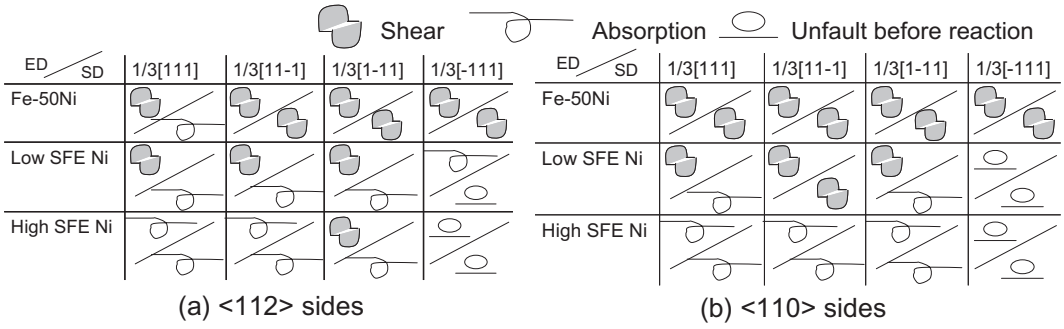

Fig. 2. The outcome of the interaction between a dislocation and Frank loop ($D_L = 4$ nm). The notation for the interaction mechanism is explained on the legend above the tables. ED and SD stand for an edge and screw dislocation, respectively. Data for 'low' and 'high' SFE Ni were obtained using the V and M potentials, respectively. The reactions were modelled at 300 K. Figs. (a and b) report the results obtained for the hexagonal loops with sides oriented along $\langle 1\,1\,2\rangle$ and $\langle 1\,1\,0\rangle$ directions, respectively.

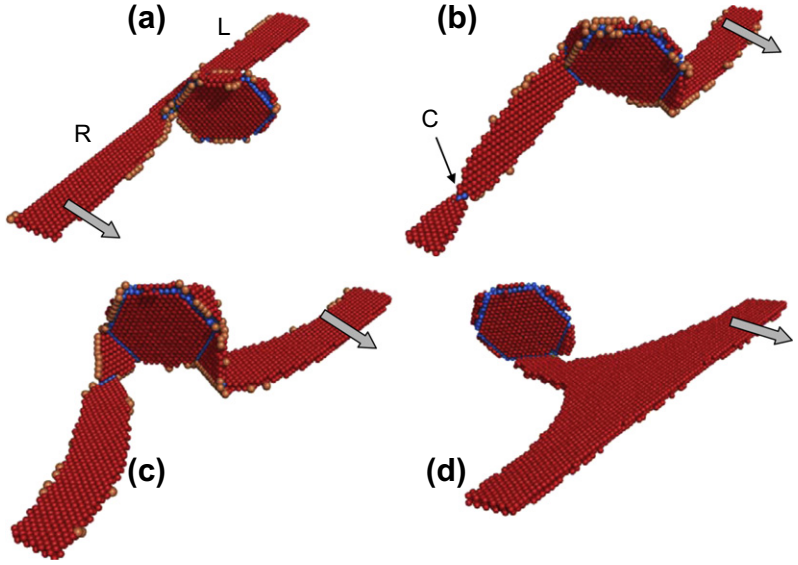

Fig. 3. Interaction of a $1/2[1\,1\,0]$ SD with a $1/3[1\,1\,\bar{1}]$ FL in Fe–50Ni at 300 K. Initially, the loop attracts the dislocation. On the contact with the loop, the dislocation forms constriction (a) and changes its glide plane from $(\bar{1}\,1\,1)$ to $(1\,\bar{1}\,1)$. Then, the left dislocation arm (labelled L) makes a second cross-slip and returns to the original glide plane (b). Now, the left arm is pinned at the front bottom corner of the loop, while the right arm is attached to the rear middle corner (b). The two arms (dissociated in different planes) are connected by the constriction (labelled C). The right arm is not glissile in the $(\bar{1}\,1\,1)$ plane and therefore only the left arm bows out under the action of increasing shear stress. This causes movement of the constriction towards the loop, thus reducing the length of the right arm on the cross-slip plane (c). Finally, the remainder of the right arm undergoes a second cross-slip so that the leading partial dislocation is completely restored (d). Now, only the trailing partial is pinned by the lower segment of the loop and final unpinning occurs via formation of a dipole and its closure. As a result, the Frank loop is fully restored, while the glide plane of the screw dislocation has been shifted down.

Please cite this article in press as: D. Terentyev et al., J. Nucl. Mater. (2013), http://dx.doi.org/10.1016/j.jnucmat.2013.01.328

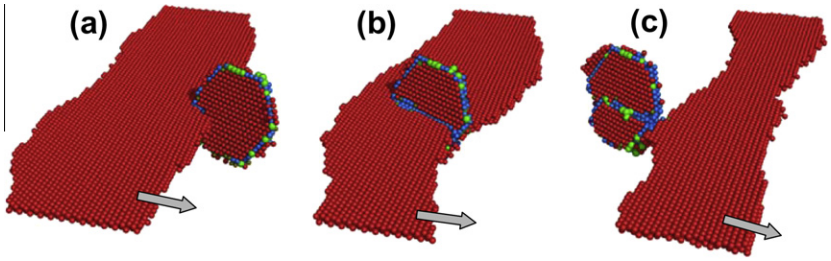

Fig. 4. Interaction of a 1/2[1 1 0] SD with a 1/3[1 1 1] FL in Fe–50Ni at 300 K. Initially, the dislocation is attracted to the loop and moves to interact with the nearest side (a). However, due to the large spacing between the partials, loop shear by the leading partial starts before a constriction can form (b). The two partials consequently shear the loop sequentially, leaving a 1/2[1 1 0] step on its surface (c).

locations. In the absence of a nearby dislocation line the same loop was observed to be stable against unfaulting at temperature up to 900 K for at least 10 ns. We therefore conclude that the nucleation of partial dislocation segments on the loop surface was induced by the stress field of the approaching dislocation. This effect was not reported in earlier studies [8,9], most probably due to the high dislocation velocity simulated there. However, loop unfaulting due to nucleation of partial dislocation segments was not observed in the reactions modelled in the Fe–50Ni alloy. These examples clearly demonstrate that a decrease of SFE suppresses the nucleation of partials on the extrinsic stacking fault and the presumed enhanced friction stress suppresses the movement of partials that could remove the stacking fault.

3.2. Effect of temperature and loop size on critical stress and interaction mechanism

To investigate the effect of loop size and temperature on loop absorption we performed a set of additional calculations at 600 K and 900 K with FLs of different sizes containing 331 (4.5 nm), 397 (5 nm), 631 (7 nm) SIAs. The goal was to see how an increase of loop size or temperature may enhance the unfaulting reaction over shear. Thus, we considered an edge dislocation and interaction geometries which at 300 K led to shear (see Fig. 2). All simulations were carried out using the V-potential for pure Ni (SFE = 58 mJ/m^2). For the loops of size 4.5 nm containing sides oriented along both ⟨1 1 0⟩ and ⟨1 1 2⟩ directions, we see that increasing temperature up to 900 K does not change the interaction mechanism. The loops were sheared. The same mechanism was observed for all the larger loops studied here. The critical resolved shear stress (CRSS or τ_C) for dislocation breakaway as a function of loop size and temperature is presented in Fig. 5. τ_C is not sensitive to simulation temperature in the case of $\boldsymbol{b} = 1/3[1\,1\,\bar{1}]$ (⟨1 1 0⟩ sides) and $\boldsymbol{b} = 1/3[1\,\bar{1}\,1]$ (⟨1 1 2⟩ sides). Whereas for other configurations, τ_C decreases with rising temperature and increases with loop size, as one would expect.

The above results also show that by increasing simulation temperature in the Fe–50Ni alloy the loop shear mechanism does not change to loop absorption. In pure metals, on the other hand, e.g. in Cu [8] and in Ni studied here, increasing temperature induced complete absorption of FLs even for an edge dislocation. The absorption occurred in a two-step reaction: (i) emergence of a screw dipole and (ii) formation of constriction on dislocation loop and cross-slip movement of the screw arms unfaulting the loop. Such mechanism has been regularly observed in pure Ni modelled using the high SFE M-potential. In contrast, in the Fe–50Ni, characterized by very low SFE, a constriction was not formed and in all cases loops were sheared before the two partials could form a constriction. This demonstrates that SFE controls the formation of constriction and activation of cross-slip, as expected, nevertheless a possible influence of enhanced friction stress in the alloys should not be forgotten.

Indeed, alloying of Fe with Ni essentially increases the friction stress for both edge and screw dislocations as compared to pure FCC metals (e.g. Ni, studied here). The mean flow stress for an edge dislocation moving in the Fe–50Ni and Fe–70Ni alloys is presented in Fig. 6. The latter was calculated by averaging the resolved shear stress while the dislocation moves with steady-state velocity of 4 m/s. We can see that in the Fe–50Ni alloy, the average flow stress is slightly lower than in Fe–70Ni, but in both cases the mean flow

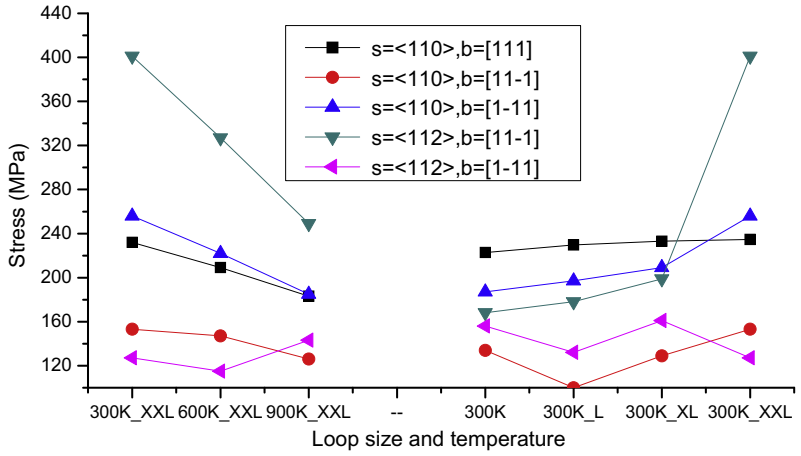

Fig. 5. CRSS in pure Ni (V potential) for an edge dislocation to unpin from Frank loops of different size. Notations L, XL and XXL stand for the loop containing 331, 397 and 631 SIAs, respectively. The orientation of the loop sides (⟨1 1 0⟩ or ⟨1 1 2⟩) and of the BV is summarized in the box.

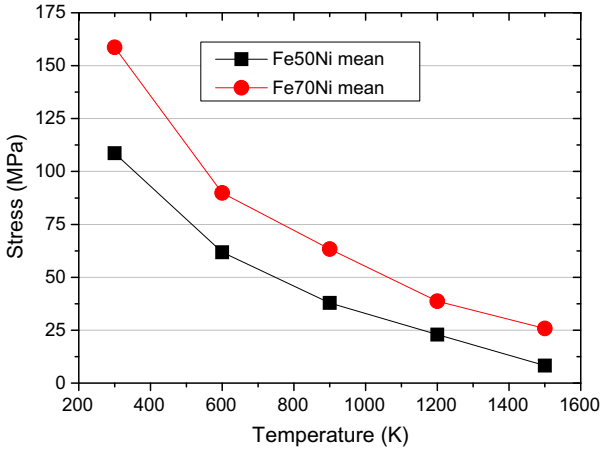

Fig. 6. Average flow stress corresponding to the movement of an edge dislocation at a speed of 4 m/s in the Fe–50Ni and Fe–70Ni alloys.

stress at $T < 1200$ K exceeds 20 MPa, which is the Peierls stress for a screw dislocation in pure Ni calculated with the V-potential at 0 K. The Peierls stress for an edge dislocation in pure Ni (4 MPa) is even lower.

To clarify the role of SFE on loop absorption in the presence of non-negligible friction stress, we have repeated a number of reactions involving an edge dislocation in Fe–70Ni (SFE = 50 mJ/m^2). While at low temperature mainly shear was observed, at high temperature (900 K) the outcome of the interactions was the same as obtained in pure Ni using the V-potential (SFE = 58 mJ/m^2). This result confirms that SFE plays a major role in the interaction process and the enhanced friction stress due to solution alloying has a secondary effect. However, a possible influence of a combination of the enhanced friction stress and variation of SFE, relevant for alloys, needs to be explored further.

4. Summary and conclusions

In this work we have studied the interaction of both edge and screw dislocations with Frank loops in pure Ni and random concentrated Fe–Ni solid solution alloys, which are characterized by low and high values of SFE in the range relevant for austenitic stainless steels. The interaction has been studied using constant strain rate loading conditions corresponding to dislocation velocity of 4 m/s. The main difference between reactions in pure Ni and the Fe–50Ni alloy was in the ability of dislocations to absorb Frank loops. In the Fe–50Ni alloy (SFE = 15 mJ/m^2) no absorption was seen in any cases involving an edge dislocation and for the screw dislocation only one configuration led to absorption. Hexagonal loops with $\langle 1\,1\,0\rangle$ sides were not absorbed under any conditions and increasing temperature up 900 K in the low SFE alloy did not modify the reaction mechanism, which was a 1/2[1 1 0] pure shear of the loop. However, in the Fe–70Ni alloy (SFE = 50 mJ/m^2) some reactions led to complete absorption at 900 K, demonstrating that SFE plays a significant role in the interaction process leading to absorption.

One also has to note that the friction stress, enhanced in the alloys by means of solid solution, suppresses the reconstruction of a sheared Frank loop, which occurs via migration of the 1/2[1 1 0] ledge formed in the shear reaction over a loop surface. In pure metals, the migration occurs rather fast, so that the planar loop surface is restored almost immediately after the interaction. However, in the alloys the restoration was seen to depend on the temperature. We therefore expect that loops can be destroyed by consequential shearing much more efficiently in alloys than in pure FCC metals. Hence, both modulation of SFE and friction stress are essential features in the determination of the reaction outcome.

Finally, a number of statements can be made based on the above summarized results:

(i) A decrease of SFE makes the formation of constrictions energetically unfavourable and hence suppresses cross-slip of screw dislocation segments, as long known from plasticity theory of FCC metals [1]. Given that in some reactions cross-slip is an essential pre-requisite for loop absorption, a decrease of SFE reduces the probability for absorption. This has been shown in the earlier studies in Ni and Cu [8,9], as well as here.

(ii) The enhanced friction stress has also been shown to suppress the absorption reaction in the case of both edge and screw dislocations. In pure Ni or Cu bowing dislocation side arms can acquire screw character and cross-slip, whereas in the alloys this process was hindered, presumably due to the friction stress in secondary glide planes. Increasing temperature, which reduces the friction stress, allows cross-slip to occur in the alloys in the same way as in pure metals.

(iii) With regard to the effect of temperature and loops size on the resistance of Frank loops against shearing, we found that some configurations are sensitive to these parameters and some not. In particular, the sensitive configurations are those where the initial interaction is repulsive (i.e. the approaching leading dislocation is repelled by the closest loop segments as determined by the mutual signs of BVs and senses of dislocation lines). In this case, the CRSS increases with loop size and decreases with temperature.

Acknowledgements

This work was performed in the framework of the EC-funded FP7/PERFORM60 project, under grant agreement 232612. Part of calculations has been performed at HPC Julich within the 'SORT' project. Research was partly supported by the Office of Fusion Energy Sciences, US Department of Energy (YNO).

References

[1] D. Hull, D.J. Bacon, Introduction to Dislocations, Butterworth-Heinemann, Oxford, 2001.
[2] S.G. Was, Fundamentals of Radiation Materials Science, Springer, New York, 2007.
[3] B.N. Singh, S.J. Zinkle, J. Nucl. Mater. 206 (1992) 212.
[4] J. Robach, I. Robertson, B. Wirth, A. Arsenlis, Philos. Mag. 83 (2003) 955.
[5] I.M. Robertson, A. Beaudoin, K. Al-Fadhalah, L. Chun-Ming, J. Robach, B.D. Wirth, A. Arsenlis, D. Ahn, P. Sofronis, Mater. Sci. Eng., A 400–401 (2004) 245.
[6] J. Robach, I. Robertson, H. Lee, B. Wirth, Acta Mater. 54 (2006) 1679.
[7] S.J. Zinkle, P.J. Maziasz, R.E. Stoller, J. Nucl. Mater. 206 (1992) 266.
[8] T. Nogaret, C. Robertson, D. Rodney, Phil. Mag. 87 (2007) 945.
[9] D. Rodney, Acta Mater. 52 (2004) 607.
[10] C. Becquart, Report F16O-CT-2003-508840, PERFECT IP Lille (2005) 22p.
[11] M. Daw, M. Baskes, Phys. Rev. B 29 (1984) 6443.
[12] T.S. Byun, Acta Mater. 51 (2003) 3063.
[13] Y. Mishin, D. Farkas, M.J. Mehl, D.A. Papaconstantopoulos, Phys. Rev. B 59 (1999) 3393.
[14] A. Voter, S. Chen, in: Mater. Res. Soc. Symp. Proc. 82, 1987, p. 175.
[15] M. Allen, D. Tildesley, Computer Simulation of Liquids, Clarendon Press, Oxford, 1987.
[16] Y.N. Osetsky, D.J. Bacon, Modell. Simul. Mater. Sci. Eng. 11 (2003) 427.